Available online at www.sciencedirect.com
ScienceDirect
Surface & Coatings Technology 201 (2006) 1845 – 1851
SURFACE & COATINGS TECHNOLOGY
www.elsevier.com/locate/surfcoat

Monte-Carlo simulation of ionisation in self-induced ion plating (SIIP)

Antonella Contino [a,*], Véronique Feldheim [a], Paul Lybaert [a], Benoît Deweer [b], Hugues Cornil [b]

[a] Faculty of Engineering Mons—Thermal Engng. and Combustion Lab., Rue de l'Epargne,56-7000 Mons—Belgium
[b] Arcelor Research Liège, Rue Sompré 1-4400 Liège—Belgium

Received 9 January 2006; accepted in revised form 8 March 2006
Available online 19 April 2006

Abstract

SIIP can be defined as the evaporation of a metallic target thanks to ion bombardment of a magnetron sputtering system. A numerical simulation model of the SIIP process has been already realized [A. Contino, V. Feldheim, P. Lybaert, B. Deweer, H. Cornil, October 2005, Modelling of continuous steel coating by self-induced ion plating (SIIP), Surface and Coatings Technology, Vol. 200, Issue 1–4, pp.898–903] in order to predict the thickness profile of the coating. The model was constituted of three coupled submodels: a magnetic model, a heat transfer model and an evaporation model. The comparison between the simulated results and the measurements showed that our results did not perfectly agree with the experimental values. This could be explained by the difficulty in doing the accurate measurements but also by simplifying assumptions introduced into the model. The purpose of the present work is to remove one of these assumptions: the use of a non-validated power law [Plasma Surface Engineering Corporation, Technology Note: Magnetron sputtering, Feb. 2003. <http//www.msi-pse.com/magnetron_sputtering.htm>] to evaluate heat flux distribution (due to ion bombardment) on the target. To obtain an accurate ion bombardment heat flux distribution we compute the ions strike points distribution on the target surface using a Monte-Carlo method [T.E. Sheridan, M.J. Goeckner, and J. Goree, 1990. Model of energetic electron transport in magnetron discharges, J. Vac. Sci. Technol. A8(1) 30–37] and we assume that the heat flux is proportional to the number of ions colliding with the target. The computed heat distribution is compared with the power-law distribution used previously. The new distribution is more accurate and will be implemented in the future in the numerical simulation model previously developed to predict coating thickness.
© 2006 Elsevier B.V. All rights reserved.

Keywords: Vacuum evaporation; Magnetron; Sputtering; Ion plating; Monte-Carlo; Ionisation

1. Introduction

Self-induced ion plating (SIIP) [1,4] is a new physical vapour deposition (PVD) process developed in order to produce a continuous coating of flat steel products. This technique is based on the two well-known PVD processes: vacuum evaporation and magnetron sputtering. SIIP presents the advantages of both techniques: the high deposition rate of the evaporation and the good adherence of the deposit layer generated by a magnetron sputtering process.

SIIP system (Fig. 1) studied in this paper is very similar to the one presented in Ref. [1]. An argon gas is ionized between a tin target at a voltage of −900 V (cathode) and a flat steel substrate at ground. The argon ions are accelerated by the electric field to the target and bombard it with a high energy. The target being not cooled, the Ar^+ bombardment does not cause the tin erosion but its melting and evaporation. The tin vapour is condensed on the substrate which has a continuous displacement with a velocity of 20 m/min at a few centimetres above the target.

A numerical simulation model of the SIIP process has been developed in a previous work [1] in order to predict the thickness profile of the coating. The SIIP simulation is based on three coupled models (magnetic model, heat transfer model and evaporation model). The comparison between the simulated results and the measurements shows that our results overestimate the experimental values. This can be explained by the difficulty in doing accurate measurements but also by simplifying assumptions introduced into the model. One of those simplifying assumptions was the use of a non-validated power law to evaluate heat distribution on target.

SIIP and sputtering process are similar except for the ion bombardment consequences: in the sputtering process the

* Corresponding author. Tel.: +32 65 374457; fax: +32 65 374400.
E-mail address: Antonella.contino@fpms.ac.be (A. Contino).

0257-8972/$ - see front matter © 2006 Elsevier B.V. All rights reserved.
doi:10.1016/j.surfcoat.2006.03.009

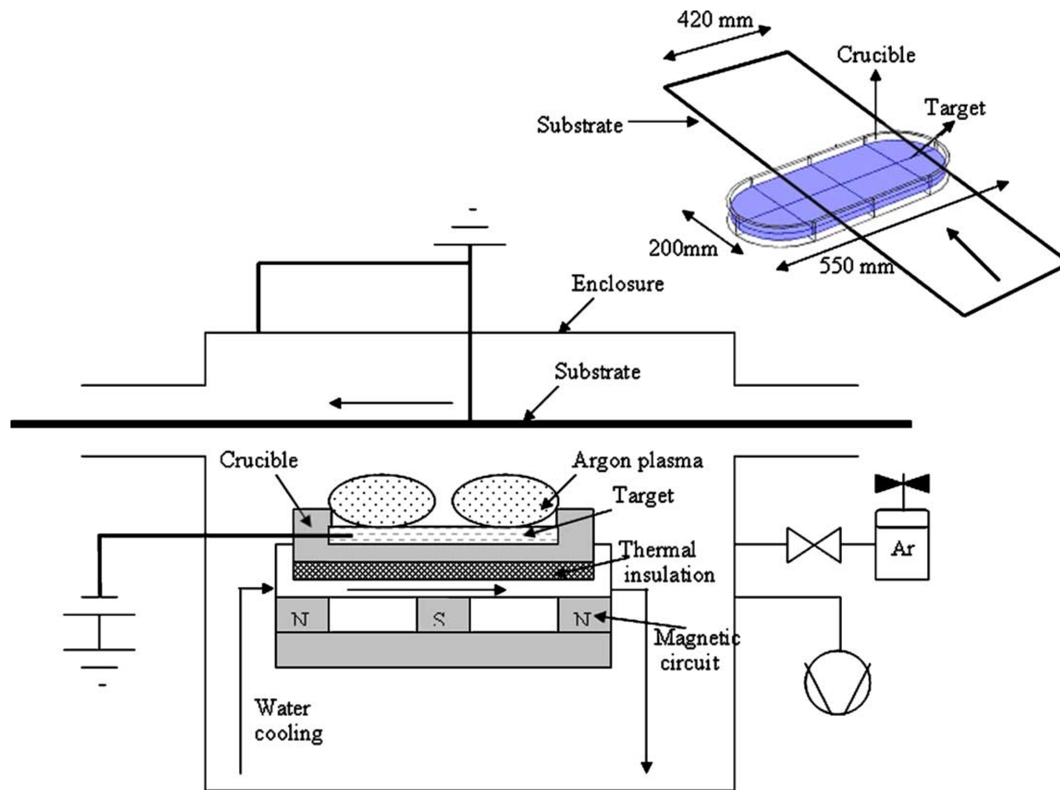

Fig. 1. SIIP Process.

target is kept solid by cooling and the ion bombardment erodes it, in the SIIP case the ion bombardment causes the target heating, melting and finally the evaporation. Because of this similarity between the SIIP and the sputtering process, we assumed that the distribution of heat flux in SIIP could be computed as an erosion profile in sputtering. In the literature, there is a lack of simple and accurate models to predict three dimensional erosion profile due to a sputtering magnetron, so we used a law presented on the Plasma Surface Engineering Corporation [2] website and validated for a two dimensional erosion profile. It claimed that the erosion depth profile in the sputtering process could be defined, using horizontal (B_{xy}) and vertical (B_z) components of magnetic induction at the target level, as

$$\left(\frac{B_{xy}}{\sqrt{B_{xy}^2+B_z^2}}\right)^3 \tag{1}$$

Thus we assumed that ion bombardment distribution was proportional to the law (Eq. (1)). Nevertheless this power law has to be validated. As Sheridan et al. [3] use the Monte-Carlo method to determine the position of ionisation sites of a magnetron sputtering system and deduce the target erosion profile from it, we decided to deduce ion bombardment heat flux distribution using the same method and compare results with distribution defined by Eq. (1). The new computed heat distribution will be introduced in the numerical simulation model previously developed.

2. Monte-Carlo method

The Monte-Carlo method is a statistical and random method which consists of following energetic electrons and defining where argon ions are created. The assumptions applied for the SIIP are: the magnetic and electric fields are time independent; electric field (E) only depends on the height above the target ($E=f(z)$); dispersion by the collisions with the neutral particles is the only mechanism of transport (turbulent transport, collective effects and collisions with the Ar^+ions are negligible); we take into account only secondary electrons (electrons emitted from the target); initial kinetic energy of the secondary electrons is supposed to be equal to zero (actually 1–4 eV); argon atom density (n_g) is uniform.

Each secondary electron emitted from the tin target is influenced by the electromagnetic field. Its trajectory is computed by numerical integration (order 4 Runge–Kutta method) of the Lorentz's law:

$$\frac{\partial \vec{v}}{\partial t}=\frac{q}{m}(\vec{E}+\vec{v}\times\vec{B}) \tag{2}$$

With q ($-1.6022\ 10^{-19}$ C) and m ($9.11\ 10^{-31}$ kg), respectively the charge and mass of electron; $\vec{v}$, the velocity (m/s); $\vec{E}$ the electric field (V/m); $\vec{B}$, the magnetic induction (T) and t, the time (sec).

At each time step of the Lorentz's law (Eq. (2)) integration, the electron is able to collide with an argon atom. The kind of

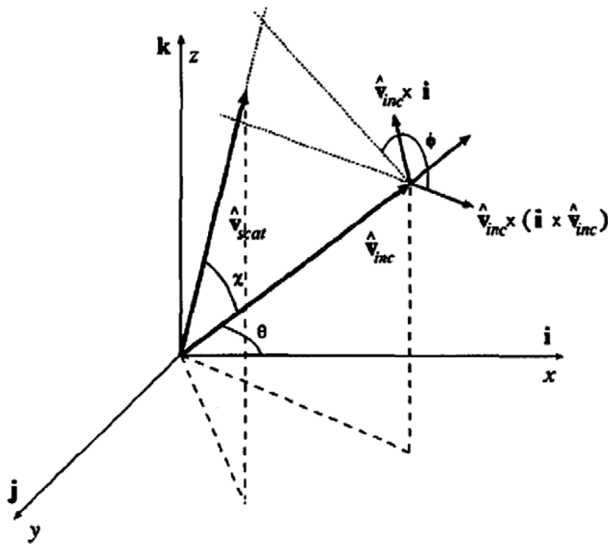

Fig. 2. Definition of incident electron scattering angles [6].

collisions taken into account are: the ionisation collision, the elastic collision or excitation collision.

To determine if a collision occurs we have to compare a random number uniformly distributed between 0 and 1 with the collision probability (P_c), defined by

$$P_c = 1 - e^{-\Delta t v \sigma_{tot}(\varepsilon) n_g} \tag{3}$$

With v, the electron velocity (m/s); $\sigma_{tot}(\varepsilon)$, the argon total collision cross section (m^2); Δt, the integration time step (s); $\varepsilon\left(\frac{mv^2}{2|q|}\right)$, the electron energy (eV) and n_g $\left(1.06\ 10^{25}\frac{p(Torr)}{T_{Ar}(K)}\right)$, the argon particle density (m^{-3}).

The total collision cross section is dependent of the electron energy ε and is the sum of the elastic, excitation and ionisation cross sections [6].

$$\sigma_{tot}(\varepsilon) = \sigma_{elastic}(\varepsilon) + \sigma_{excitation}(\varepsilon) + \sigma_{ionisation}(\varepsilon) \tag{4}$$

If the random number R is greater than the collision probability P_c, there is no collision and we have to integrate the Lorentz's law for the next step. If R is smaller than P_c, we conclude that there is a collision between electron and argon. So the next step is to define which kind of collision (ionisation, elastic or excitation) it is. In order to define the kind of electron–argon collision, we have to generate a new random number R_1 uniformly distributed between 0 and 1 and we compare it with the relative probabilities:

$$P_{elast} = \frac{\sigma_{elast}(\varepsilon)}{\sigma_{tot}(\varepsilon)}; P_{excit} = \frac{\sigma_{elast}(\varepsilon) + \sigma_{excit}(\varepsilon)}{\sigma_{tot}(\varepsilon)}; P_{ion} = \frac{\sigma_{elast}(\varepsilon) + \sigma_{excit}(\varepsilon) + \sigma_{ion}(\varepsilon)}{\sigma_{tot}(\varepsilon)} = 1$$
$$0 \le R_1 < P_{elast} \rightarrow \text{Elastic}; P_{elast} \le R_1 < P_{excit} \rightarrow \text{Excitation}; P_{excit} \le R_1 < P_{ion} = 1 \rightarrow \text{ionisation} \tag{5}$$

If the collision is an ionisation one, we record the spatial coordinates (x,y,z) of the ionisation site.

When an electron undergoes a collision, its energy (and velocity value) and direction are modified. We assume that the energy of incident electron does not decrease if the collision is an elastic one and decreases of 15.8 eV and 11.6 eV for respectively ionisation and excitation collisions. We assume that the scattering of incident electron direction after the collision [6] is the same for all kinds of collision. The scattering angle χ (Fig. 2) is defined using:

$$\cos\chi = \frac{2 + \varepsilon - 2(1+\varepsilon)^{R_2}}{\varepsilon} \tag{6}$$

With R_2, a random number uniformly distributed in the interval [0,1].

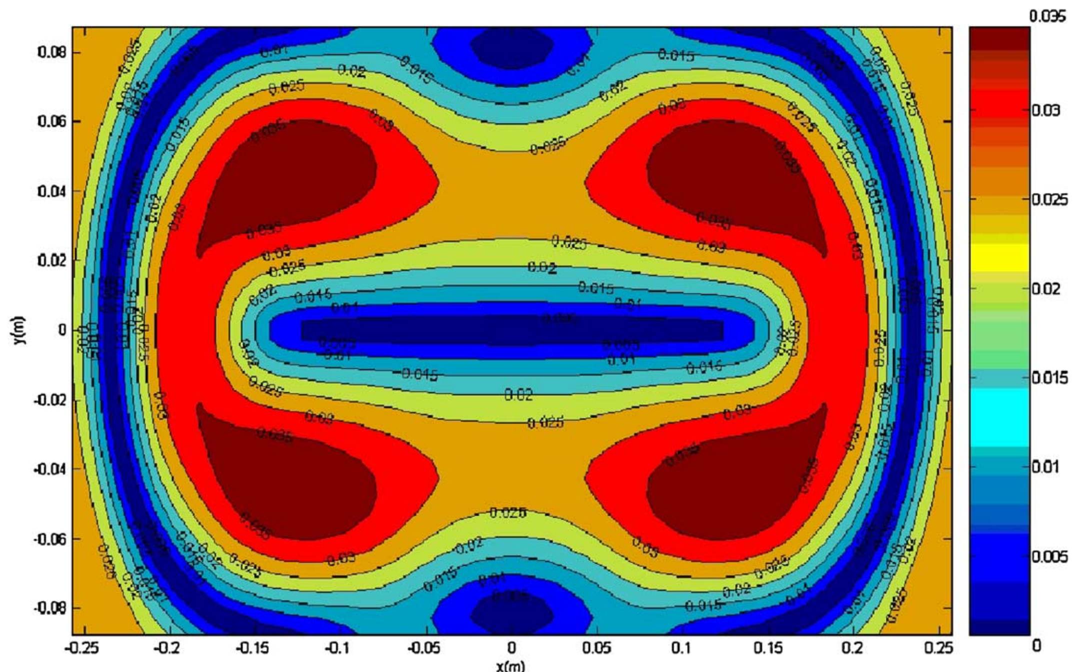

Fig. 3. Absolute value of horizontal component of magnetic induction (Tesla).

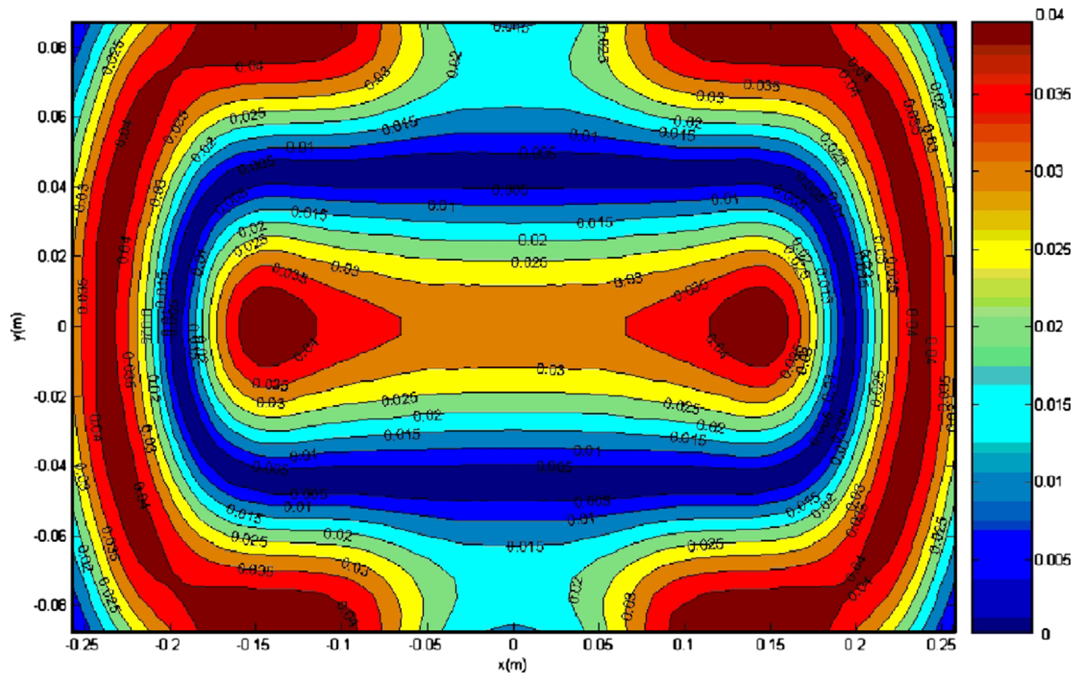

Fig. 4. Absolute value of vertical component of magnetic induction (Tesla).

The azimutal scattering angle ϕ is uniformly distributed in the interval [0,2π]. ϕ is defined thanks to

$$\Phi = 2\pi R_3 \tag{7}$$

With R_3, a random number uniformly distributed in the interval [0,1].

Thanks to the scattering angles χ (Eq. (6)) and ϕ (Eq. (7)) and considering the angle θ between the incident velocity (v_{inc}) direction and x axis (Fig. 2), we can compute the scattered direction (v_{scat}) of electron using:

$$v_{scat} = v_{inc}\cos\chi + v_{inc} \times i\frac{\sin\chi\sin\Phi}{\sin\theta} + v_{inc} \times (i \times v_{inc})\frac{\sin\chi\sin\Phi}{\sin\theta} \tag{8}$$

This new velocity (new direction, new value) is used as initial velocity for the next integration step of the Lorentz's law (Eq. (2)).

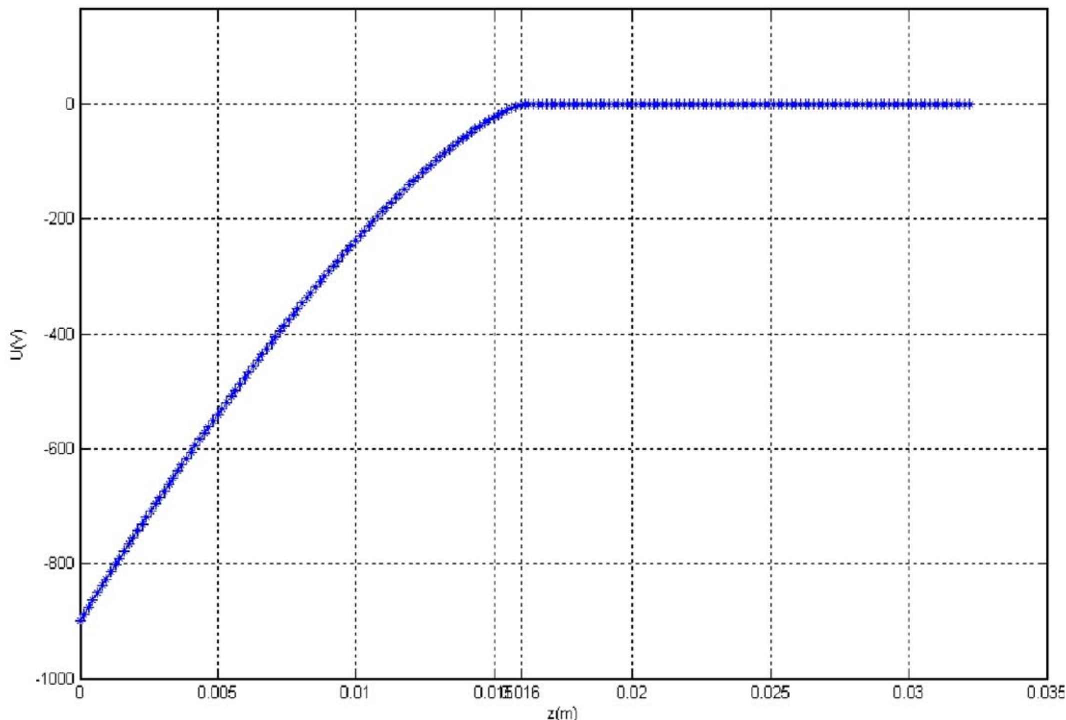

Fig. 5. Potential in the cathode sheath for SIIP.

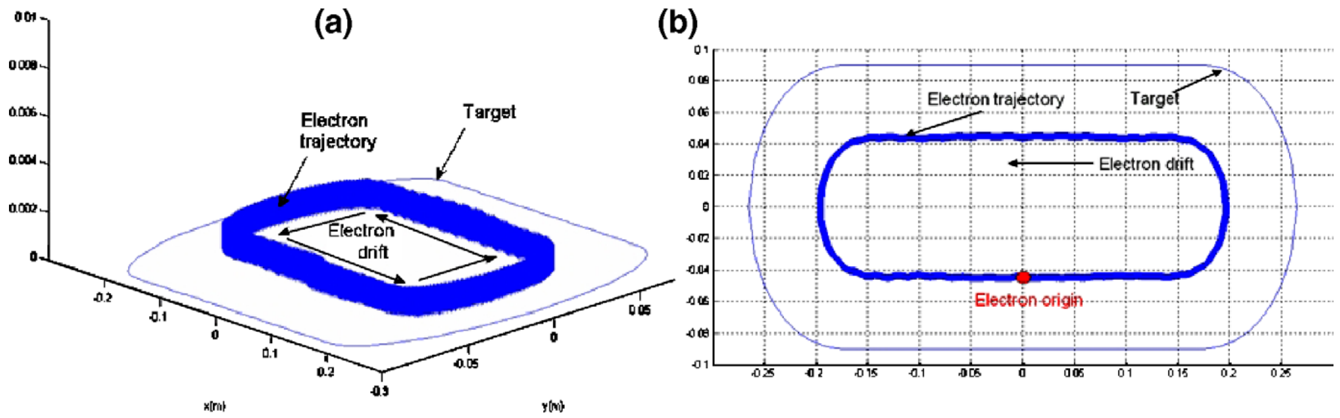

Fig. 6. An example of electron trajectory above the target surface: (a) three-dimensional view; (b) top view.

We follow a secondary electron until one of those events occurs: the electron leaves of the simulation zone; the electron energy becomes lower than ionisation potential.

Except for the first secondary electron which is emitted from a random position on the target, the other electrons are assumed to be created from the projection of ionisation sites on target.

3. Monte-Carlo simulation of ionisation in SIIP

To apply the Lorentz's law (Eq. (2)) to the SIIP, we need to know the magnetic field and electric field distribution above the tin target. The magnetic field induced by permanent magnets of the magnetron is computed using the magnetostatic laws and the finite element software FEMLAB® [1,5]. We can see on Figs. 3 and 4, respectively the horizontal and vertical components (in absolute value) of magnetic induction at the target level. On Fig. 4 we can note the position of the zone where a magnetic field is parallel to the target surface. This zone is important because we know that the maximal heat flux obtained using Monte-Carlo should have to be concentrated there.

The electric field in the cathode sheath is computed using the analytical model presented by Sheridan and Goree in Ref. [7]. Fig. 5 shows the evolution of the electrical potential with the height above the tin target. We can see that the cathode sheath is 16 mm wide.

Using a 4th order Runge–Kutta method with a time step Δt of 10^{-11} s, we integrate the Lorentz's law (Eq. (2)) to compute electron trajectory. Fig. 6 shows an electron trajectory example where collisions are not taken into account. The electron is emitted from a target position where magnetic field is tangential to the target. We can note the electron drift effect.

Considering elastic, excitation and ionisation collisions, we obtain the ions distribution as presented in Fig. 7 for 34,000 secondary electrons followed from the target. Fig. 8 shows the projection of ionisation sites on the target. We can see the ions concentration around the zone where the magnetic field is parallel to the target.

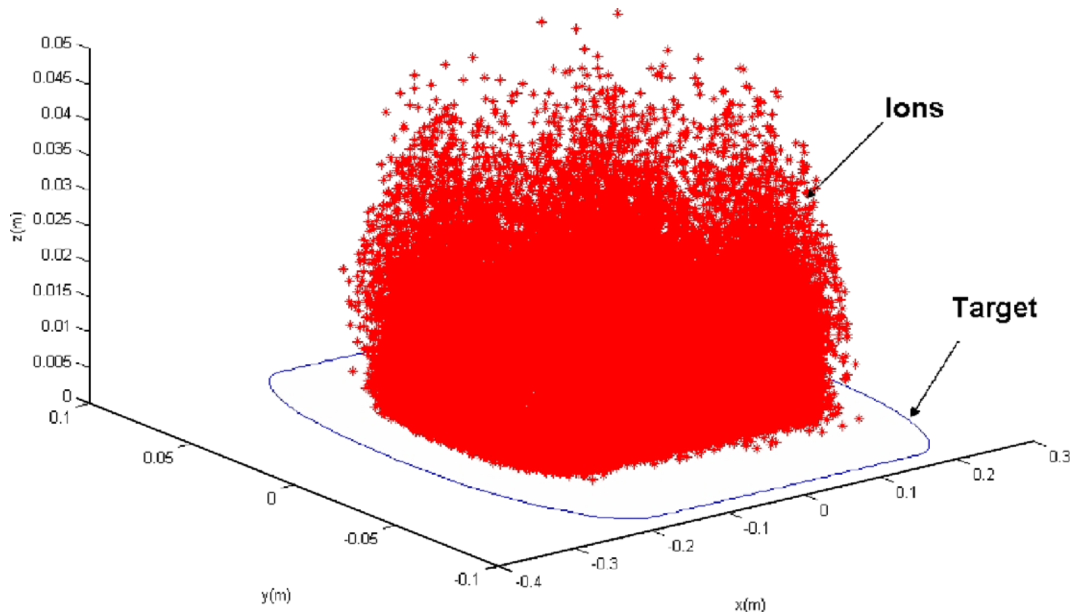

Fig. 7. Ions distribution (in the (x,y,z)) space.

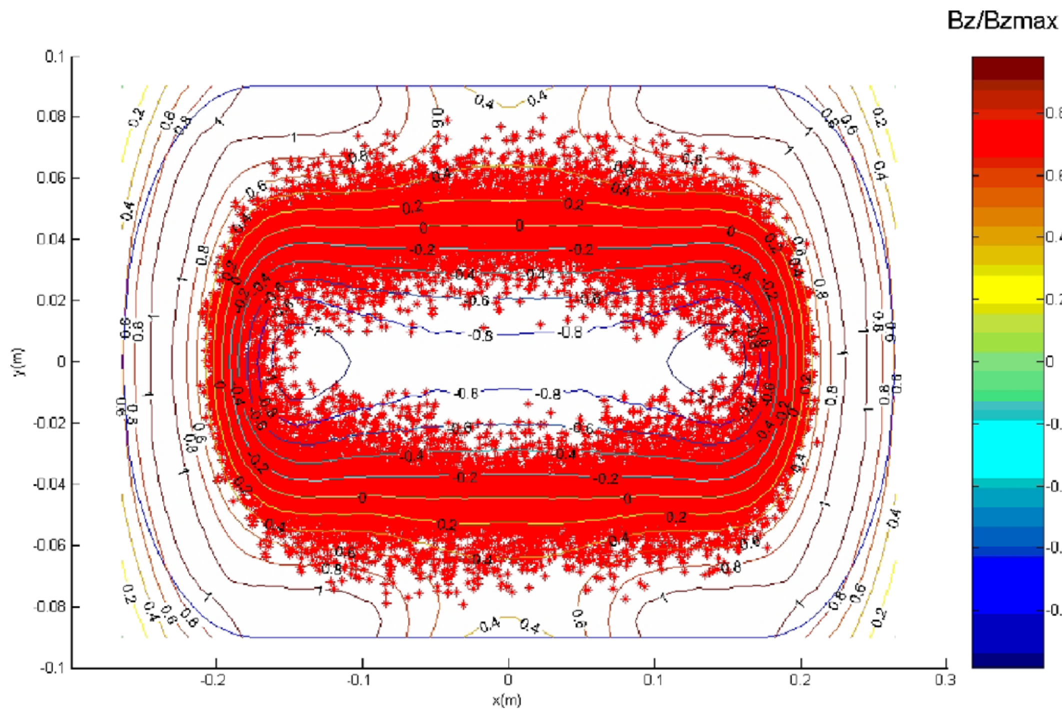

Fig. 8. Projection on the target surface of the ions distribution and normalised value of the vertical component of the magnetic induction.

We assume that the ions distribution on the target is very similar to the heat distribution of ion bombardment. In fact, when ions are created, they fall down to the target without being scattered by a magnetic field. Fig. 9 shows this normalised ion bombardment heat distribution.

If we compare Fig. 9 with Fig. 10 where the heat flux distribution (Eq. (1)) previously used is drawn, we can see that the distributions are very different. The result presented in Fig. 9 is better. In fact, in Ref. [8], Shidoji et al. notice that an anomalous erosion occurs at the boundary of the straight section and the curve section in a rectangular magnetron sputtering system. This anomalous erosion appears where the horizontal magnetic field is greater than 0,02 T and in the presence of a local weak horizontal magnetic field at the curved section (compared to the straight section). Given the similarity between the classical magnetron sputtering method and the SIIP, we can

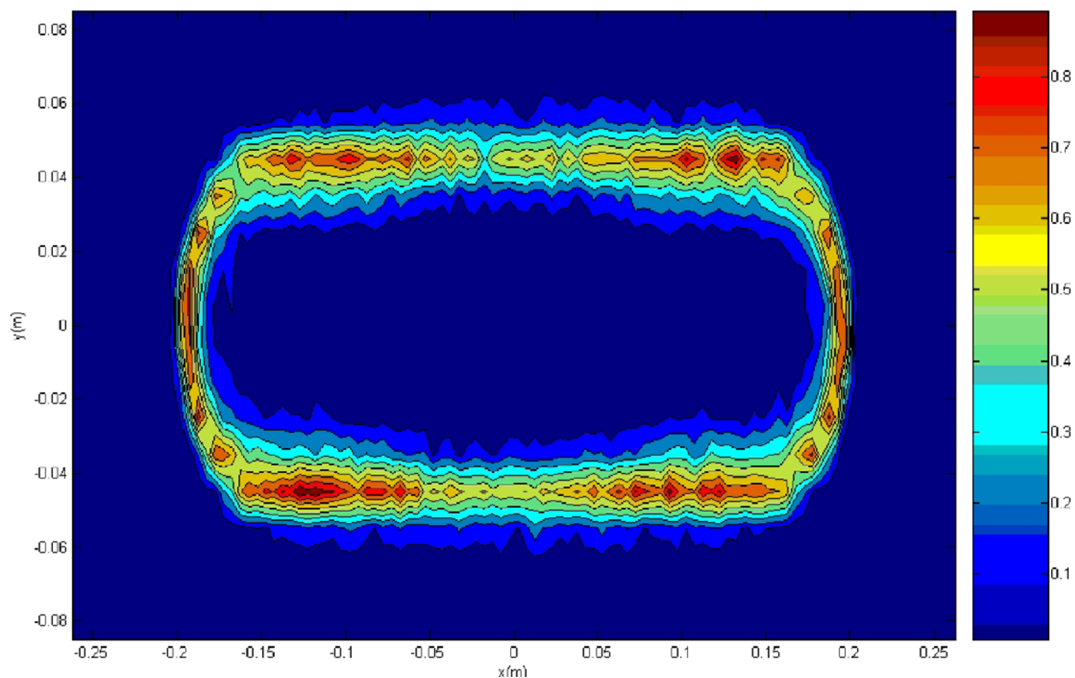

Fig. 9. Normalised ion bombardment heat flux distribution.

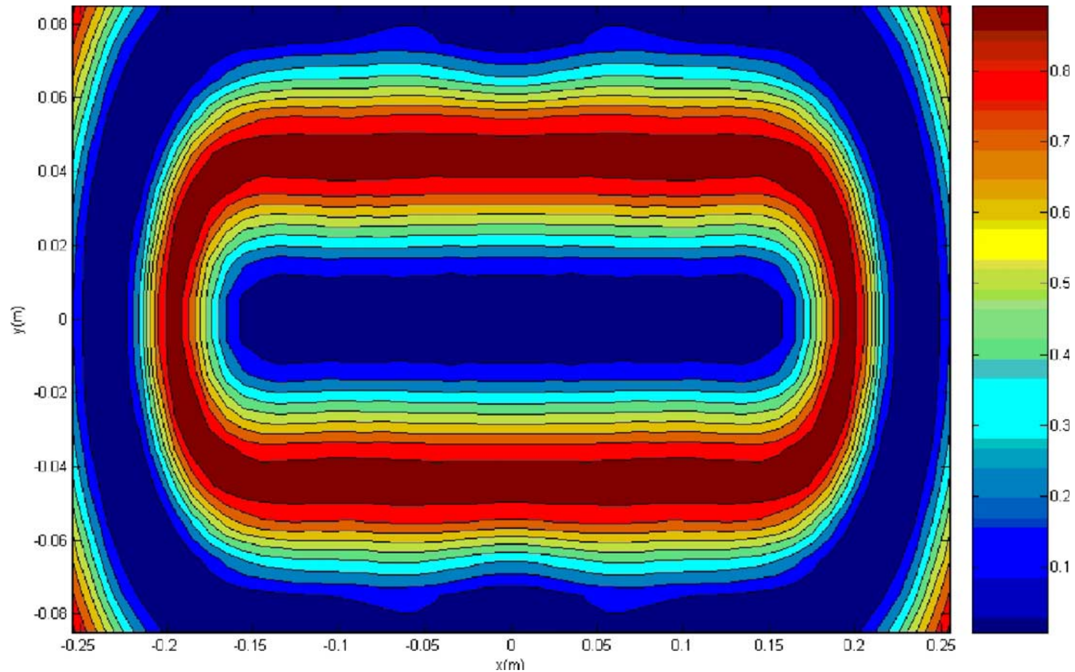

Fig. 10. Normalised distribution used in Eq. (1) for the SIIP.

explain the four zones (Fig. 9) where ion heat flux distribution is greater by the local difference of the horizontal magnetic induction value (Fig. 3) between the straight and the curved zone. This new ion bombardment heat flux distribution deduced from the ions distribution computed by the Monte-Carlo method will have to be introduced in the simulation model of the SIIP [1] to obtain more accurate results.

4. Conclusions

The aim of the present work was to remove an assumption applied to the SIIP simulation model presented in [1]. We have to compute the heat distribution (due to ion bombardment) on target more accurately than using the empirical law (Eq. (1)). Given the similarity between the classical magnetron sputtering and the SIIP, we employ a Monte-Carlo method to compute ion strike points distribution and deduce from it the ion bombardment heat flux distribution. The heat distribution so computed is compared with the power-law used previously. The new distribution is more accurate and shows a maximum of the heat flux between the straight and the curved zone of the target. These observations are validated in experiments by Shidoji et al. in Ref. [8]. This accurate heat flux distribution will have to be introduced in the future in the numerical simulation model developed previously to predict coating thickness.

References

[1] A. Contino, V. Feldheim, P. Lybaert, B. Deweer, H. Cornil, Surf. Coat. Technol. 200 (1–4) (October 2005) 898.
[2] Plasma Surface Engineering Corporation, Technology Note: Magnetron sputtering, Feb. 2003. Available from Internet: <http// www.msi-pse.com/magnetron_sputtering.htm>.
[3] T.E. Sheridan, M.J. Goeckner, J. Goree, J. Vac. Sci. Technol. A8 (1) (1990) 30.
[4] P. Vanden Brande, S. Lucas, A. Weymeersch, European Patent N° 0780489 (Nov. 1996).
[5] Femlab 3.1 Documentaion, Comsol Inc., 2004.
[6] V. Vahedi, M. Surendra, Comput. Phys. Commun. 87 (1995) 179.
[7] T.E. Sheridan, J. Goree, IEEE Trans. Plasma Sci. 17 (6) (1989) 884.
[8] E. Shidoji, M. Nemoto, T. Nomura, J. Vac. Sci. Technol., A 18 (6) (2000).